Experiments and Theory on the Thermal Decomposition of $CHCl_3$ and the Reactions of CCl_2

S. S. Kumaran,[†] M.-C. Su,[‡] K. P. Lim, J. V. Michael,* and S. J. Klippenstein[§]

Chemistry Division, Argonne National Laboratory, Argonne, Illinois 60439

J. DiFelice, P. S. Mudipalli, and J. H. Kiefer*

Department of Chemical Engineering, University of Illinois at Chicago, Chicago, Illinois 60680

David A. Dixon*

Environmental Molecular Sciences Laboratory, Pacific Northwest National Laboratory, P.O. Box 999, Richland, Washington 99352

Kirk A. Peterson

Chemistry Department, Washington State University, Pullman, Washington 99164, and Environmental Molecular Sciences Laboratory, Pacific Northwest National Laboratory, P.O. Box 999, Richland, Washington 99352

Received: May 29, 1997[⊗]

Rate constants for the thermal decomposition of $CHCl_3$ in Kr diuent have been measured by the laser schlieren density gradient method. The only decomposition process indicated is molecular elimination giving the singlet carbene, CCl_2, and HCl. Rate constants are determined under different conditions of density over the temperature range 1282−1878 K, giving $k(\pm 15\%) = 4.26 \times 10^{16} \exp(-22\,516\ \mathrm{K}/T)\ \mathrm{cm^3\ mol^{-1}\ s^{-1}}$. Electronic structure calculations have provided models for both the transition state and molecule. With these models, both semiempirical Troe and Rice−Ramsperger−Kassel−Marcus unimolecular theoretical calculations are carried out. The experimental results agree with theory provided $E_0 = 56.0$ kcal mol^{-1} and $\langle \Delta E \rangle_{\mathrm{down}} = (820 \pm 30)$ cm^{-1}, suggesting that the barrier for back reaction is 3.8 kcal mol^{-1}. Cl-atom atomic resonance absorption spectrometric (ARAS) experiments, also in Kr diluent, are then carried out, confirming that atom formation is entirely due to the thermal reactivity of CCl_2. On the basis of Cl-atom yield measurements, a mechanism for Cl-atom formation is devised. Chemical simulations of the absolute Cl-atom profile data then provide estimates of the temperature dependences for the rate constants used in the mechanism. These results are discussed in terms of unimolecular reaction rate theory suggesting that the heat of formation for CCl radicals is 100 ± 4 kcal mol^{-1} at 0 K. Our calculated results (R-CCSD(T)) extrapolated to the complete basis set limit give values of $\Delta_f H^0_{\mathrm{CCl_2,0K}} = 53.0$ and $\Delta_f H^0_{\mathrm{CCl,0K}} = 102.5$ kcal mol^{-1} and are consistent with the experimental results reported herein. Additionally, the results suggest that CCl_2 undergoes dissociative recombination with a substantial activation energy.

Introduction

Following earlier experimental studies on the thermal decompositions of halogen-substituted methanes from these laboratories,[1−3] and also from Argonne alone,[4−11] we report dissociation rate constants for the thermal decomposition of $CHCl_3$ in this paper. In many chlorofluoromethanes, thermal dissociation involves only C−Cl bond fission;[1,2,4,7,9] however, with hydrogen substitution in chloromethanes, molecular elimination producing HCl and a singlet carbene diradical can compete with bond fission;[3,5,12] i.e., for $CHCl_3$,

$$CHCl_3\ (+\ M) \rightarrow CCl_2 + HCl\ (+\ M) \qquad (1a)$$

$$\rightarrow CCl_2H + Cl\ (+\ M) \qquad (1b)$$

In two early studies,[13,14] reaction (1b) was considered to be the major dissociation pathway. There are other investigations of note,[15,16] but in all of these studies, the reaction progress was complicated by wall reactions. It now seems clear from the work of Schug et al.,[12] Herman et al.,[17] Shilov and Sabirova,[18] and Won and Bozzelli,[19] however, that reaction (1a) dominates the dissociation. Herman et al. studied the reaction in a molecular beam apparatus. Schug et al. studied the decomposition in a shock tube experiment between 1050 and 1380 K. They suggested that the CCl_2 from (1a) subsequently recombined to form C_2Cl_4, and the temporal optical absorption of C_2Cl_4 was then used to estimate rate constants for the thermal dissociation, (1a). They reported a calculated high-pressure rate constant, $k_{1\infty} = 1.8 \times 10^{14} \exp(-27\,423\ \mathrm{K}/T)\ \mathrm{s^{-1}}$. CCl_2 recombination to give C_2Cl_4 has been confirmed in one pyrolytic and two incineration studies.[19−21] In the pyrolytic study,[19] (1b) was also found to be negligible in comparison to (1a), and they reported $k_{1\infty} = 1.6 \times 10^{14} \exp(-28\,183\ \mathrm{K}/T)\ \mathrm{s^{-1}}$ for $808 \le T \le 1073$ K at 1atm Ar.

Based on recent thermochemical estimates,[10,22−24] the reaction endothermicities at 0 K for reactions (1a) and (1b) are (52.2 ± 2.0) and (77.5 ± 1.0) kcal mol^{-1}, respectively. To our

[†] Present address: Cabot Corporation, 700 E. US Highway 36, Tuscola, IL 61953.

[‡] Sabbatical Leave. Permanent address: Department of Chemistry, Butler University, Indianapolis, IN 46208.

[§] Sabbatical Leave. Permanent address: Department of Chemistry, Case-Western Reserve University, Cleveland, OH 44106.

[⊗] Abstract published in *Advance ACS Abstracts,* October 15, 1997.

S1089-5639(97)01723-4 CCC: $14.00

knowledge, there are no reported studies on the reverse of the elimination process (i.e., the reaction of singlet carbene with HCl), and therefore, the presence of a potential energy barrier for the reverse process, (−1a), is uncertain.

In the present study, the laser schlieren (LS) technique has been used to measure the total endothermic decomposition rate of $CHCl_3$ in incident shock waves between 1282 and 1878 K. In addition, Rice−Ramsperger−Kassel−Marcus (RRKM) modeling of the rate constants has been accomplished using ab initio results for the transition state. The Cl-atom atomic resonance absorption spectrometric (ARAS) technique has subsequently been used to examine Cl-atom formation. The interesting issues are (a) whether formation by reaction (1b) can become competitive with (1a) under any conditions or, (b) if (1b) is insignificant, whether the results involve secondary CCl_2 reactions, similar to those recently documented for CFCl from the thermal decomposition of $CFCl_3$.[9]

Experimental Section

Laser Schlieren (LS) Technique. The shock tube and associated LS equipment have been described in detail.[25] All measurements were made in the incident wave.

Apparatus. Shock waves were generated by a spontaneous burst of Mylar diaphragms with helium. Incident velocity at the observation window (He−Ne laser beam) was determined through interpolation from four arrival intervals established by five piezoelectric detectors feeding a four-channel, 10 MHz clock. The uncertainty in velocity was estimated as ±0.3% based on the consistency of interval measurements and corresponds to a ΔT of about ±10 K at 2000 K. Raw data are angular beam deflections, θ, that are derived from the detector signals with the usual rotating-mirror calibration of angular sensitivity.[25] The final stage in the initial analysis of raw data is the conversion of these deflection signals to density gradient profiles through $\theta = KW\, d\rho/dx$, where W is the tube diameter and K is the specific mixture refractivity.[25]

Gases. Experiments were performed in 1 and 4% $CHCl_3$ dilute in Kr. $CHCl_3$ (99.9+%) was obtained from Aldrich and Kr (99.997%) from Spectra-Gases. Both were used without purification. Mixtures were prepared manometrically with MKS capacitance manometers having a stated accuracy of 0.5%. Test gas was stored in a 50 L glass bulb, and mixed with a Teflon-coated magnetic stirrer. Refractivities were atomic and assumed to be constant.

Cl-Atom ARAS Technique. These experiments used a shock tube apparatus operating in the reflected wave regime. The experimental methods and techniques have already been documented;[26,27] therefore, only those procedures relevant to this study are described.

Apparatus. The shock tube equipment was used as described previously.[26,27] Reaction mixtures were prepared manometrically with an MKS Baratron capacitance manometer. Initial reactant loading pressures were measured with the same manometer. Experiments in three different $CHCl_3$−Kr mixtures were performed behind reflected shock waves. The average incident shock velocity for each experiment was measured with fast piezoelectric transducers (PCB Piezotronics, Inc., Model 113A21), and the reflected shock regime thermodynamic properties were calculated from the velocities with appropriate Mirels' boundary layer corrections as described earlier.[26,28,29] Cl-atoms were observed as a product from the pyrolysis of $CHCl_3$ with a Cl-atom ARAS photometer system that has an optical path length of 9.94 cm. Transmittances from the resonance lamp were measured with a solar blind EMR G14 photomultiplier tube, and the signals were processed using a Nicolet 4094C digital oscilloscope.

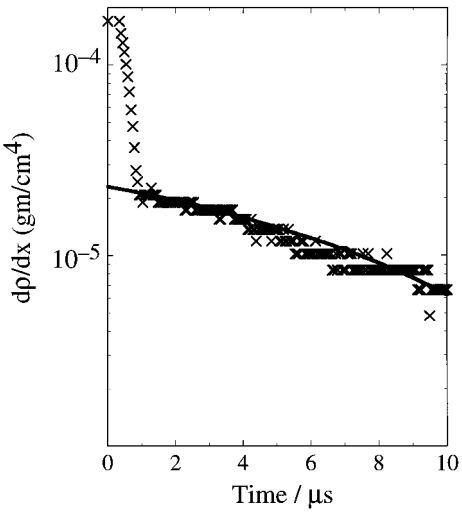

Figure 1. Laser schlieren (LS) experiment in 4% $CHCl_3$−Kr. The symbols (×) are measured density gradients, $d\rho/dx$. Postshock frozen-reaction conditions are $T_2 = 1344$ K, $\rho_2 = 1.739 \times 10^{18}$ molecules cm^{-3}. The solid line is the model-calculated fit to the experimental data using the mechanism of Table 1.

Cl-Atom ARAS Detection. The Cl-atom ARAS technique for time-resolved Cl-atom detection has already been described.[1−7,9] The resonance lamp operates at 50 W microwave power in a 2.0 Torr flowing mixture of $X_{Cl_2} = 10^{-3}$ in He. As discussed by Clyne and Nip[30] and Whytock et al.,[31] this source gives a multiplet structure that is somewhat reversed. The resonance radiation is observed through a BaF_2 filter without wavelength resolution over the range 133.6−139.6 nm. From pyrolytic studies of CCl_4,[1] this lamp configuration yields (14 ± 2)% nonresonance radiation. Thus, unambiguous determination of $(ABS)_{Cl} \equiv -\ln(I/I_0)$ can be made as a function of [Cl] in experiments where complete dissociation is obtained. Experiments with a variety of Cl-atom thermal sources[2,4,6,32] has allowed for the determination of the curve-of-growth. On the basis of near linear behavior for $(ABS)_{Cl} \leq 0.1$, the effective Cl-atom absorption cross section is $(2.37 \pm 0.08) \times 10^{-15}$ cm^2. However, the curve-of-growth becomes nonlinear at $(ABS)_{Cl} > 0.1$ and is best represented by a modified Beer's law expression

$$(ABS)_{Cl} = 4.41 \times 10^{-9}\,[Cl]^{0.582} \qquad (2)$$

where [Cl] is expressed in atoms cm^{-3}.[6]

Gases. The He driver gas (99.995%) was obtained from Air Products and Chemicals, Inc. Diluent Kr used in the reaction mixture was Scientific grade (99.997%) from MG Industries. Electronic grade Cl_2 (99.999%) from MG Industries, diluted in Scientific grade He (99.9999%) from MG Industries, was used in the Cl-atom resonance lamp. $CHCl_3$ at 99.9% was obtained from Aldrich Chemical Co. and was purified by bulb-to-bulb distillation. The middle third was retained for mixture preparation.

Results

$CHCl_3$ Decomposition with LS. Figure 1 shows an LS experiment obtained with relatively high density and $[CHCl_3]_0$, but at relatively low temperature, *T*. By contrast, Figure 2 shows two experiments at lower density and $[CHCl_3]_0$, but at higher *T*.

TABLE 1: Mechanism for the Thermal Decomposition of $CHCl_3$ over the Range $1200 \leq T \leq 2700$ K

reaction[a]	log A[b]	n	E_a	source
(1a) $CHCl_3$ (+ Kr) → CCl_2 + HCl (+ Kr)	16.6	0	44.7	PW
(2) $CCl_2 + CCl_2 = C_2Cl_2 + Cl + Cl$[c]	14.7	0	15.2	PW
(3) $CCl_2 + Kr \rightarrow CCl + Cl + Kr$	27.0	−3.047	79.8	RRKM, PW
or	15.6	0	67.6	fit, see text
(4) $CCl_2 + CCl_2 + Kr \rightarrow C_2Cl_4 + Kr$[d]	15.1	0	−12.6	RRKM est
(5) $HCl + Kr \rightarrow H + Cl + Kr$	14.7	0	81.0	ref 33
(6) $Cl + CHCl_3 \rightarrow CCl_3 + HCl$	13.3	0	2.7	ref 34
(7) $CCl_3 + CCl_2 \rightarrow C_2Cl_4 + Cl$	12.0	0	0	est
(8) $CCl_3 + CCl_3 = C_2Cl_4 + Cl + Cl$[c]	12.0	0	0	est
(9) $CCl_3 + Kr \rightarrow CCl_2 + Cl + Kr$	16.2	0	48.4	ref 1
(10) $Cl_2 + Kr \rightarrow Cl + Cl + Kr$	14.0	0	50.0	ref 35
(11) $CCl + CCl = C_2 + Cl + Cl$[c]	13.3	0	0	PW
(12) $C_2Cl_2 = C_2 + Cl + Cl$	16.0	0	67.8	PW

[a] Reverse rate constants for each reaction are included. [b] Rate constants of the form, log k(cm^3/mol s) = log A − n log T − E_a (kcal mol^{-1})/2.303RT. [c] An equals sign denotes the overall process involving the initial formation of a radical + Cl followed by the subsequent very fast dissociation of the radical to give a product and another Cl atom. [d] Termolecular rate constant in cm^6/mol^2 s.

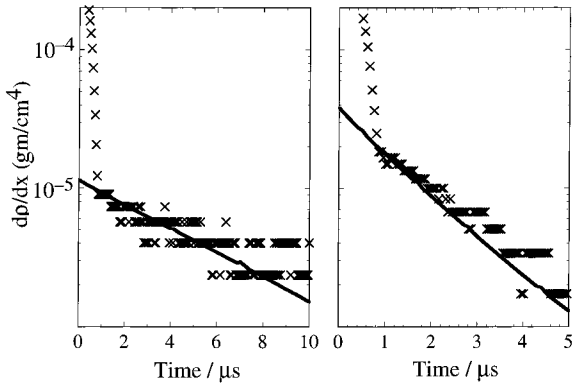

Figure 2. Laser schlieren (LS) experiments in 1% $CHCl_3$−Kr. The symbols (×) are measured density gradients, dρ/dx. Postshock frozen-reaction conditions are (left) $T_2 = 1613$ K, $\rho_2 = 0.611 \times 10^{18}$ molecules cm^{-3}; (right) 1805 K, $\rho_2 = 0.615 \times 10^{18}$ molecule cm^{-3}. The solid lines are the respective model-calculated fits to the experimental data using the mechanism of Table 1.

The dρ/dx profiles measure the total endothermic rates as a function of time, and the value of dρ/dx at $t = 0$ is solely due to the dissociation of $CHCl_3$. Since a small portion of the initial gradient immediately behind the shock front cannot be observed, this initial gradient requires an extrapolation of 0.5−1.0 μs to $t = 0$. At short times the gradient is still mainly caused by simple dissociation, and the magnitude of dρ/dx is determined by its rate constant and the endothermicity for dissociation. Preliminary analysis with kinetics modeling of the $CHCl_3$ LS data indicated that the measured dρ/dx requires a dissociation rate that is consistent with $\Delta H^0_{1a,0K} = 52.2$ kcal mol^{-1}, the known enthalpy change for reaction (1a).[22−24] Below 1900 K, there was no need to include reaction (1b) in the analysis, suggesting that it is negligible in comparison to (1a). In the initial stages of reaction, the gradient is dominated by simple dissociation, and the determination of dρ/dx is unambiguous, particularly at lower T (Figure 1). However, modeling of the higher T late-time gradients requires a knowledge of the secondary chemistry, and therefore, a more complete mechanism is needed in order to give both a reliable extrapolation to $t = 0$ and a better fit to the late-time gradients. A 10-step trial mechanism used for modeling the experiments is given in Table 1 as reversible reactions (1)−(10).

The solid lines in Figures 1 and 2 were calculated using the 10-reaction mechanism. Within about the first 5 μs, the calculations were only sensitive to the rate of reaction (1a); the effects of secondary chemistry are always slight and are only seen at longer times. The calculation may therefore be used to extrapolate back to $t = 0$ quite accurately, providing initial dissociation rate constants for the unimolecular elimination of HCl. The experimental conditions and derived second-order rate constants for (1a) are given in Table 2 and are plotted in Figure 3. The results can be expressed to within ±15% at the one standard deviation level by the Arrhenius expression

TABLE 2: Laser Schlieren Kinetics Results for the $CHCl_3$ Decomposition

P_2 (Torr)[a]	ρ_2 (10^{18} molecule cm^{-3})[a]	T_2 (K)[a]	k_{1a} (10^{10} cm^3 mol^{-1} s^{-1})[b]
	$X_{CHCl_3} = 1.00 \times 10^{-2}$		
101.6	0.594	1651.1	5.07
102.0	0.611	1612.7	4.89
103.6	0.539	1858.0	21.1
103.8	0.577	1736.1	11.5
105.1	0.641	1583.5	3.40
106.0	0.634	1614.8	3.39
107.5	0.654	1587.1	3.50
108.4	0.560	1868.0	28.0
108.5	0.674	1554.7	2.64
109.6	0.592	1786.8	13.7
111.3	0.572	1878.1	23.5
111.7	0.691	1561.8	2.62
115.0	0.615	1804.5	17.0
117.9	0.658	1730.5	9.69
119.9	0.650	1781.4	14.5
121.3	0.768	1524.8	1.84
123.0	0.681	1743.5	10.7
127.2	0.731	1681.7	6.43
207.6	1.136	1764.5	9.69
209.9	1.177	1722.6	7.44
210.3	1.225	1657.7	4.82
215.2	1.274	1631.0	3.81
226.0	1.378	1584.2	2.51
228.8	1.426	1549.4	2.24
235.2	1.481	1534.1	1.90
235.8	1.570	1450.3	0.881
243.4	1.621	1449.9	0.768
250.8	1.720	1408.5	0.516
261.3	1.819	1387.0	0.418
	$X_{CHCl_3} = 4.00 \times 10^{-2}$		
137.7	0.957	1390.0	0.478
230.5	1.578	1411.0	0.506
231.7	1.514	1478.0	0.946
240.4	1.687	1376.0	0.342
242.0	1.739	1344.0	0.221
251.4	1.894	1282.0	0.108
263.1	1.962	1295.0	0.137
336.9	2.293	1419.0	0.436
348.5	2.418	1392.0	0.204
365.3	2.647	1333.0	0.173

[a] Quantities with the subscript 2 refer to the thermodynamic state of the gas in the incident shock region. [b] The rate constants are derived as described in the text.

TABLE 3: Cl-Atom Kinetics Results from $CHCl_3$ Decomposition

P_1[a]	M_s[b]	ρ_5[a]	T_5/(K)[a]	k_2[c]	k_3[c]	k_4[c]	k_{11}[c]	k_{12}
				$X_{CHCl_3} = 2.112 \times 10^{-5}$				
15.96	2.329	2.842	1376	3.0 (12)		7.3 (16)		
15.96	2.515	3.061	1578	3.6 (12)	1.97 (6)	2.5 (16)	1.8 (13)	3.94 (6)
15.88	2.687	3.225	1777	5.4 (12)	9.34 (6)		1.8 (13)	1.87 (7)
15.92	2.815	3.354	1933	6.6 (12)	9.88 (7)		1.8 (13)	1.98 (8)
15.94	2.321	2.829	1368	2.4 (12)		7.3 (16)		
15.82	2.157	2.590	1202	6.0 (11)		7.3 (16)		
15.92	2.190	2.652	1234	1.5 (12)		3.6 (16)		
5.94	2.972	1.317	2163	3.0 (13)	6.86 (8)		1.8 (13)	1.33 (9)
5.91	3.142	1.363	2401	3.6 (13)	3.09 (9)		3.6 (13)	6.19 (9)
5.94	3.155	1.374	2420	2.4 (13)	2.19 (9)		4.8 (13)	4.38 (9)
5.94	2.828	1.267	1972	1.7 (13)	2.14 (8)		3.0 (13)	4.28 (8)
5.85	2.743	1.216	1863	6.6 (12)	1.49 (8)		3.0 (13)	2.97 (8)
5.96	2.526	1.149	1601	3.6 (12)				
5.94	2.363	1.071	1417	2.4 (12)		3.6 (16)		
5.94	2.218	1.000	1259	3.3 (12)		7.3 (16)		
5.89	2.304	1.036	1349	1.6 (12)		7.3 (16)		
				$X_{CHCl_3} = 2.599 \times 10^{-6}$				
15.90	2.937	3.455	2089	1.8 (13)	2.61 (8)		1.8 (13)	5.23 (8)
15.95	2.925	3.444	2081	1.8 (13)	2.62 (8)		1.8 (13)	5.25 (8)
15.88	2.525	3.047	1595	3.0 (12)	2.96 (6)	1.8 (16)	1.8 (13)	5.93 (6)
15.91	2.680	3.214	1776	6.0 (12)	1.87 (7)		1.8 (13)	3.75 (7)
16.00	2.778	3.325	1894	5.4 (12)	8.15 (7)		1.8 (13)	1.63 (8)
15.93	2.823	3.375	1937	6.6 (12)	1.43 (8)		1.8 (13)	2.86 (8)
15.95	3.010	3.536	2178	2.4 (13)	6.81 (8)		1.8 (13)	1.33 (9)
15.90	2.583	3.123	1655	3.0 (12)	1.93 (6)	7.3 (16)	1.8 (13)	3.86 (6)
15.94	2.705	3.255	1798	6.6 (12)	2.78 (7)		1.8 (13)	3.70 (7)
				$X_{CHCl_3} = 1.013 \times 10^{-6}$				
15.98	2.722	3.269	1826	8.4 (12)	7.37 (7)		1.8 (13)	1.84 (8)
15.95	2.931	3.449	2089	1.2 (13)	4.80 (8)		1.8 (13)	1.05 (9)

[a] Quantities with the subscripts 1 and 5 refer to the thermodynamic state of the loading gas and the gas in the reflected shock region, respectively. P is in Torr and ρ is in 10^{18} molecules cm^{-3}. [b] The error in measuring the Mach number, M_s, is typically 0.5−1.0% at the 1 standard deviation level. [c] The rate constants are derived as described in the text (parentheses denote the power of ten). k_2, k_3, k_{11}, and k_{12} are in second-order units, cm^3 mol^{-1} s^{-1} while k_4 is in third-order units, cm^6 mol^{-2} s^{-1}. All rate constants refer to the reactions listed in Table 1.

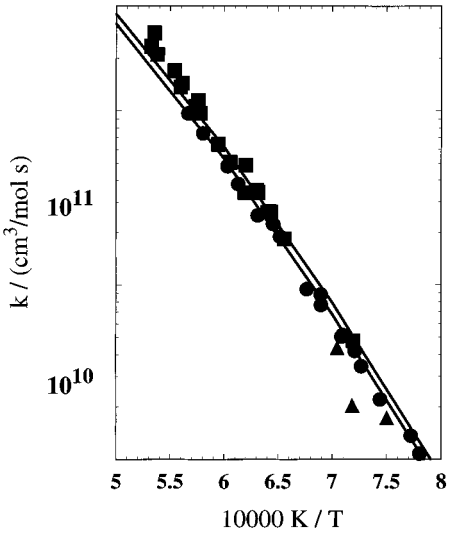

Figure 3. Arrhenius plot of measured (second-order) rate constants for $CHCl_3$ (+ Kr) → CCl_2 + HCl (+ Kr), using the LS technique, over 1282−1878 K (Table 2). The postshock pressure ranges are (■) 103−137 Torr, (●) 208−263 Torr, and (▲) 337−365 Torr. The solid lines show the spread in RRKM (method 2)-predicted rate constants for the lower and upper pressure ranges. These calculations were carried out with $E_0 = 56.0$ kcal mol^{-1} and $\langle \Delta E \rangle_{down} = 850$ cm^{-1} using the Table 4 ab initio properties (see text).

$$\log k_1/(\mathrm{cm^3\ mol^{-1}\ s^{-1}}) = 16.63 - 44.74\ \mathrm{kcal/mol}/2.303RT \quad (3)$$

between 1282 and 1878 K.

Although the extrapolation to $t = 0$ is quite unambiguous with the mechanism of Table 1, the mechanism does not contain all the reactions needed to model late-time density profiles for high initial concentrations and high temperatures. Several experiments were performed with 4% $CHCl_3$ (diluted with Kr), which exhibit a change from positive density gradients (endothermic processes) to negative density gradients (exothermic processes) and then back again to positive gradients. This behavior qualitatively suggests that substantial CCl_2 secondary chemistry may be occurring. This secondary CCl_2 chemistry is not included in the primary mechanism presented in Table 1 but will be further examined in the ARAS experiments.

Cl-Atoms from the $CHCl_3$ Dissociation. Thirty-seven Cl-atom ARAS experiments were performed between 1202 and 2729 K at two loading pressures and three mole fractions (21.12, 2.60, and 1.01 ppm) of $CHCl_3$ using previously described methods.[1−7,9] The conditions of 27 of these are given Table 3. Using the full mechanism of Table 1 and the value for k_{1a} from eq (3), we determined that for $T \geq 1350$ K, initial decomposition in the ARAS experiments was so fast that subsequent Cl-atom formation was entirely due to the reactions of CCl_2. Under the Table 3 conditions, all secondary reactions, (5) to (10) in Table 1, are therefore negligible. Hence, it was necessary to postulate additional processes involving CCl_2 in order to explain the results.

The minimum mechanism necessary to rationalize the data was deduced from the following observations. (a) Cl-atoms were observed in experiments with 21.12 ppm $CHCl_3$ and 322 Torr at temperatures as low as 1202 K; however, the profiles (not shown) were strongly concave upward (i.e., not first-order). At 1202 K, C_2Cl_4, from reaction (4) in Table 1 is surely a product,[19−21] but the C−Cl bond is too strong for direct CCl_2 dissociation. Hence, we conclude that Cl must be formed by dissociative recombination of CCl_2 (reaction (2) in Table 1)

giving $C_2Cl_3 + Cl$. The C_2Cl_3 radicals then dissociate rapidly to give the final overall products, $C_2Cl_2 + 2Cl$. Balancing the competition between stabilization and decomposition of the initially formed vibrationally hot C_2Cl_4 molecule (reactions (4) vs (2)) must then be an element in the explanation of the low T Cl-atom profiles. (b) Under about the same total pressure conditions but with $2100 \leq T \leq 2700$ K and 1.01 ppm $CHCl_3$, the observed yield of Cl-atoms, $[Cl]_\infty/[CHCl_3]_0$, was less than or equal to unity. With ~20 times less $CHCl_3$ and at high T, it is doubtful that reaction (2) in Table 1 can compete effectively with direct CCl_2 dissociation (reaction (3) in Table 1) which produces Cl + CCl. Diatomic CCl is stable[22] and would not be expected to appreciably dissociate. Hence, this scheme provides the observed yields only if CCl is removed slowly, the slow process postulated as being dissociative CCl recombination (ultimately giving $C_2 + 2Cl$, reaction (11) in Table 1). (c) Lastly, with 21.16 ppm and ~300 Torr at $2150 \leq T \leq 2400$ K, the overall yield of Cl-atoms was ~2. If CCl_2 dissociative recombination dominates at this higher $[CHCl_3]_0$, then the yield suggests that the product, C_2Cl_2, must itself undergo thermal decomposition, and therefore, we postulate the overall reaction (12) in Table 1. With this expanded mechanism (reactions (1)−(4), (11), and (12) in Table 1), the ARAS experiments of Table 3 were fitted, and the rate constants listed in the table were thereby determined.

Discussion

The Thermal Decomposition of $CHCl_3$. The present results summarized by eq (3) cannot be directly compared to the earlier results[12,18,19] because of different ranges of pressure and temperature; however, comparison is possible provided the present results can be theoretically described. We have accordingly applied two versions of unimolecular rate theory using ab initio electronic structure determinations for both the transition state and molecule.

Following recent work from this laboratory,[10] the second-order dissociation rate constants have been theoretically modeled with semiempirical Troe and RRKM calculations. Both methods include appropriate weak collision corrections through the efficiency factor, β_c, set by the average energy transfer parameter, $\langle\Delta E\rangle_{down}$. The input data used for the two methods was obtained as follows. The $CHCl_3$ equilibrium and HCl-elimination transition-state geometries and frequencies were initially determined at the Hartree−Fock level with a DZP basis set on the singlet energy surface. With the same basis set, these geometries were used as starting structures in MP2 optimizations for the final determination of geometries and frequencies.[36] Starting from a single-configuration wave function, this approach is valid for the process even though only singlet CCl_2 is considered (the triplet is neglected due to the large singlet−triplet splitting). After scaling by 0.96, the calculated zero-point energy decreased 4.9 kcal mol^{-1} in going from equilibrium $CHCl_3$ to the transition state. These final frequencies and the moments of inertia from the computed geometries are listed in Table 4. The reaction barrier at the MP2/DZP transition-state location was reevaluated with more complete basis set and correlation calculations at the MP4(SDTQ)/TZ2PF and at the CCSD(T)/CC levels (CC corresponds to a correlation consistent basis set).[36] Including the 4.9 kcal mol^{-1} zero-point energy correction, the best theoretical value for the reaction barrier is 55.9 kcal mol^{-1} (Table 4) obtained at the CCSD(T)/CC level.[37] The molecular quantities in Table 4 were then used in the two theoretical models for describing the dissociation rate data.

The first theoretical model (method 1) uses the semiempirical method of Troe[38−41] to determine the pressure and temperature behavior for the rate constants. This type of calculation uses the Whitten−Rabinovitch method for calculating the density of states and is fully described elsewhere.[9] Method 2 is a full RRKM calculation that has also been detailed.[9] A standard falloff calculation of the unimolecular rate constant as a function of pressure is carried out with numerical integration over energy. Weak collision effects are accounted for as in method 1.

TABLE 4: Ab Initio Molecular Parameters and RRKM Calculated Results for the Dissociation: $CHCl_3$ (+ Kr) → CCl_2 + HCl (+ Kr)

Ab Initio Results: $E_0 = 55.9$ kcal mol^{-1}

species	scaled freq/ cm^{-1} [a]	moments of inertia (10^{-38} g cm^2/molec)
$CHCl_3$	3117, 1233, 1233, 775, 775, 666, 364, 261, 261	2.576(2), 4.965
$[CCl_2-HCl]^‡$	1253, 1148, 885, 774, 587, 343, 176, 85, 520 *i*	2.396, 4.65, 6.943

RRKM Calculations (1300−1900 K): $E_0 = 56.0$ kcal mol^{-1}

high-pressure limit. $\log(k_\infty/s^{-1}) = 15.21-58.97$ (kcal mol^{-1})/(2.303RT)
low-pressure limit.

method	$\log\left(\frac{A_0}{\text{cm}^3\ \text{mol}^{-1}\ \text{s}^{-1}}\right)^b$	n_0	T_0	$\langle\Delta E\rangle_{down}$/ cm^{-1}
1	51.75	9.92	33480	787
2	50.18	9.50	32536	850

[a] Scaling factor is 0.96. [b] $k_0 = A_0\ T^{-n_0} \exp(-T_0/T)$.

As recently demonstrated,[3] it is always best to have an independent and reliable experimental estimate of the threshold energy, E_0. As mentioned above, low-temperature data on this dissociation[18] have been obtained between 783 and 857 K at total pressures of ~15−30 Torr $CHCl_3$ or in the presence of toluene. Hence, these data are almost certainly strong collision results (i.e., $\beta_c = 1.0$). Therefore, in unimolecular theoretical descriptions, they may be more sensitive to E_0 than the shock tube data. Using the Table 4 input parameters with either method, the theoretical preditions are low by only ~10% compared to those reported by Shilov and Sabirova[18] provided $E_0 = 55.0$ kcal mol^{-1}. Because of the relatively low pressure range, the data are, however, only between 25 and 30% of the high-pressure limit.

When $E_0 = 55.0$ kcal mol^{-1} is used for describing the present data with method 1, the rate constant at 1600 K requires $\langle\Delta E\rangle_{down} = 650$ cm^{-1}; however, the temperature dependence is not well predicted, being 21% too high at 1300 K and 33% too low at 1900 K. However, in complete agreement with the ab initio value, we found that $E_0 = 56.0$ kcal mol^{-1} and $\langle\Delta E\rangle_{down} = 787$ cm^{-1} gave the best agreement. The results are summarized in Table 4. The RRKM calculations (method 2) likewise required $E_0 = 56.0$ kcal mol^{-1}; however, the necessary value for $\langle\Delta E\rangle_{down}$ was 850 cm^{-1}. The predicted high-pressure limits are identical since the transition state and threshold energy are the same with either method. The results of this calculation are also summarized in Table 4 and are shown as solid lines in Figure 3 for two densities used in the present experiments. The weak pressure dependence observed in the experiments is well predicted with this theoretical model.

Even though the inferred values for $\langle\Delta E\rangle_{down}$ are slightly different using the two methods, the results are indistinguishable. Despite higher temperatures in our experiments than those of Shilov and Sabirova,[18] the calculations indicate that the present data are actually closer to the high-pressure limit (i.e., within

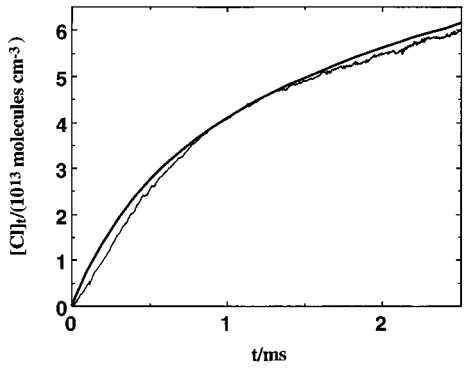

Figure 4. A comparison between a typical experimental $[Cl]_t$ profile and a simulation using the mechanism of Table 1. The experimental conditions are $T = 1777$ K and $\rho = 3.225 \times 10^{18}$ molecule cm^{-3} at $X_{CHCl_3} = 2.112 \times 10^{-5}$. The rate constants are given in the third entry in Table 3.

31−58%). Therefore, our estimate, $E_0 = 56.0$ kcal mol^{-1}, is preferred since the present results are more sensitive to E_0. If this value is adopted along with $\Delta H^0_{1a,0K} = 52.2$ kcal mol^{-1} (implied by JANAF[22] and Kohn et al.[24]), then the barrier for back-reaction (−1a) is 3.8 kcal mol^{-1}, a value similar to that for $CF_2 + HCl$ (2.8 kcal mol^{-1}).[3] For comparison, the theoretical result is discussed in ref 37.

We have additionally tried to rationalize the shock tube results of Schug et al.;[12] however, our rate constant predictions for their conditions with $E_0 = 56.0$ kcal mol^{-1} and $\langle\Delta E\rangle_{down} = (820 \pm 30)$ cm^{-1} are roughly one-half of their measurements. They assumed that CCl_2 was completely converted to C_2Cl_4, but we have shown that Cl-atoms will undoubtedly be a product under their conditions. Hence, we suggest that the mechanism used by them in the rate constant analysis was incomplete. Won and Bozzelli's flow tube experiments and calculations allowed them to estimate the high-pressure rate constant as $k_{1a\infty} = 1.6 \times 10^{14} \exp(-28\,183\ K/T)$ s^{-1} for $808 \le T \le 1073$ K at 1 atm Ar. Our $k_{1a\infty}$ in Table 4 is 2−3 times larger over the same T-range, no doubt due mostly to the differences in transition states. However, these authors[19] report the experimental rate constant for their T-range and 1 atm Ar in their Table 11 as $k_{1a} = 5.2 \times 10^{12} \exp(-25\,918\ K/T)$ s^{-1}. This expression gives respective values at 808 and 1100 K, 0.61 and 304 s^{-1}. Application of the present theory (Table 4) for their conditions gives 0.68 and 309 s^{-1}, respectively. Hence, we fully agree with the results of Won and Bozzelli provided $\langle\Delta E\rangle_{down}$ is the same in Ar and Kr. We would further suggest that these results are only between 10 and 32% of the high-pressure limit even at 1 atm Ar and $808 \le T \le 1073$ K.

Cl-Atom Formation from CCl_2. Using the model of Table 4, theoretical extrapolations to the conditions of the ARAS experiments then supplied values for k_{1a}. We then attempted to fit the Cl-atom profile data by varying the rate constants for reactions (2)−(4), (11), and (12) in Table 1, giving the results listed in Table 3. A typical fit is shown in Figure 4. It should be emphasized that this procedure in no way determines a unique mechanism that is both necessary and sufficient. For example, several profiles could be better reproduced by excluding one or more of the considered reactions; however, application of the reduced mechanism to other conditions of density and temperature then gave totally inconsistent values for some of the rate constants. One could also suggest that this 6-step mechanism is incomplete, and Won and Bozzelli[19] have already suggested several other processes that might be considered. However, under the high T and low $[CHCl_3]_0$ conditions of the ARAS experiments, most of these processes can be ruled out.

The quality of the fits for the 27 experiments reported in Table 3 is fair. Between 200 μs and 2 ms, the predicted Cl-atom profiles with the listed rate constants are within ±10% in 13, ±16% in 8, and ±25% in 6 of the absolute measurements. We view this level of agreement to be satisfactory since, at 1 standard deviation error, (a) the absolute [Cl] from eq (2) is only accurate to within ±8%,[4,6,32] and (b) the error in T_5 and ρ_5 due to uncertainties in velocity measurements are ∼±1.5% and 0.8% of the respective values shown in the table.[27−29]

We are therefore suggesting that the relative importance of different mechanistic pathways changes substantially over the full range of T, ρ, and $[CHCl_3]_0$ probed in this study. Under all conditions the initial dissociation gives only $CCl_2 + HCl$. At low temperatures and high pressures, CCl_2 can only recombine to give C_2Cl_4 (reaction (4) in Table 1). However, at about 1200−1300 K, dissociative recombination starts to compete with stabilization. As temperature increases, CCl_2 unimolecular dissociation giving $CCl + Cl$ (reaction (3) in Table 1) can occur at the expense of bimolecular dissociative recombination, particularly at lower $[CHCl_3]_0$. At the highest temperatures, the Cl-atom yields can become either 1 or 2 depending on $[CHCl_3]_0$, which in turn dictates the extent of bimolecular vs unimolecular CCl_2 destruction. In this view, we have to postulate that (a) $2CCl \rightarrow C_2Cl + Cl$ is slow (reaction (11) in Table 1) but that (b) $C_2Cl_2 \rightarrow C_2Cl + Cl$ is fast (reaction (12) in Table 1). In both cases, $C_2Cl \rightarrow C_2 + Cl$ would have to be fast.

The T-dependence of the Table 3 rate constants can be used to discuss some important implications. Linear least-squares fits of the values in the table give the second-order Arrhenius expressions

$$k_2 = 5.4 \times 10^{14} \exp(-7641\ K/T)\ \text{cm}^3\ \text{mol}^{-1}\ \text{s}^{-1} \quad (4)$$

$$k_3 = 4.4 \times 10^{15} \exp(-34\,014\ K/T)\ \text{cm}^3\ \text{mol}^{-1}\ \text{s}^{-1} \quad (5)$$

$$k_{11} = 2.2 \times 10^{13}\ \text{cm}^3\ \text{mol}^{-1}\ \text{s}^{-1} \quad (6)$$

$$k_{12} = 9.3 \times 10^{15} \exp(-34\,134\ K/T)\ \text{cm}^3\ \text{mol}^{-1}\ \text{s}^{-1} \quad (7)$$

and the third-order expression

$$k_4 = 5.7 \times 10^{15} \exp(2993/T)\ \text{cm}^6\ \text{mol}^{-2}\ \text{s}^{-1} \quad (8)$$

The question as to whether the speculations summarized by eqs (4)−(8) (which refer to reactions (2)−(4), (11), and (12) in Table 1) are reasonable, can now be addressed.

In an earlier paper on the decomposition of $CFCl_3$,[9] the competition between dissociative recombination and direct dissociation of CFCl was described. In contrast to the present CCl_2 case, both processes could be time-resolved under differing experimental conditions. Rate constants for the thermal dissociation of CFCl using low-pressure RRKM theory with $E_0 =$ ∼81 kcal mol^{-1} [22] and $\langle\Delta E\rangle_{down} = 1000$ cm^{-1} were estimated as $2.14 \times 10^{15} \exp(-36\,183\ K/T)$ cm^3 mol^{-1} s^{-1}. The analogous CCl_2 result, eq (5), gives values ∼10 to 20 larger for CCl_2 decomposition, suggesting that the threshold value for this radical is lower than that for CFCl. However, the E_0 implied by the JANAF tables[22] and Kohn et al. ($\Delta_f H^0_{CCl_2,0K} = (50.7 \pm 2.0)$ kcal mol^{-1})[24] is 97.0 kcal mol^{-1}. We note that with this C−Cl bond strength in CCl_2 it would simply be impossible to ever approach a yield of unity at 2100−2700 K under low $[CHCl_3]_0$ conditions. Hence, given the $\Delta_f H^0_{CCl_2,0K}$ from Kohn et al., the experimental results suggest that the heat of formation given by JANAF for CCl must be in error. The arguments are

TABLE 5: R-CCSD(T) Bond Dissociation Energies for $X^2\Pi$ CCl and X^1A_1 CCl_2

basis	$D_e(CCl)^a$	$D_0(CCl)$	$D_e(CCl_2)$
cc-pVDZ	82.82	81.60	68.43
cc-pVTZ	90.79	89.56	74.37
cc-pVQZ	94.31	93.06	77.21
cc-pV5Z	96.14	94.89	
CBS limit (eq (9))	97.0	95.7	79.1

[a] All energies in kcal mol^{-1}

unchanged if the slightly higher value (51.8 ± 3.4 kcal mol^{-1}) from Paulino and Squires is used.[23] We therefore initially estimated the zero-point energy corrected threshold energy for reaction (3) in Table 1 by using the G2(MP2) ab initio method,[42] and the value obtained was $E_0 = 79.6$ kcal mol^{-1}. This value is 17 kcal mol^{-1} smaller than the JANAF and Kohn et al. implication, suggesting again, from both and experimental and theoretical points of view, that the JANAF $\Delta_f H^0_{CCl,0K}$ must be wrong.

To obtain a better value for $\Delta_f H^0_{CCl,0K}$, we carried out further more accurate ab initio electronic structure calculations at the CCSD(T) level[43] with the correlation consistent basis sets (cc-pVxZ where x = D, T, Q, 5) that have been developed by Dunning and co-workers.[44] The advantage of using these basis sets is that properties such as the bond energy, bond distance, and frequency converge to the complete basis set (CBS) limit for a given level of correlation energy treatment.[44] Other work has shown that the CCSD(T) level provides an excellent treatment of the correlation energy.[43] The calculations were done with the program MOLPRO[45] at the R-CCSD(T) level[46] (valence electrons correlated unless specified below) for the $X^2\Pi$ state of CCl. The bond energies as a function of basis set are shown in Table 5 and are plotted in Figure 5. An exponential extrapolation of the form[47]

$$F(n) = F_{CBS} + B\exp(-Cn) \qquad (9)$$

(with n = 2, 3, 4, and 5 for DZ, TZ, QZ, and 5Z sets) was used to obtain convergence to the complete basis set limit. The bond energy was obtained based on an extrapolation of the total energies. The calculations converge to a complete basis set value of 97.0 for D_e and to a value of 95.7 kcal mol^{-1} for D_0. Because CCl contains a second-row atom, it is possible that core−valence correlation effects may need to be considered. To estimate the size of the core−valence correlation effects, calculations were done with the new polarized weighted core−valence correlation consistent basis sets (cc-pwCVTZ and cc-pwCVQZ) developed by Dunning and co-workers[48] at the R-CCSD(T) level. At the cc-pwCVTZ level, the value of D_e increases by 0.38, and at the cc-pwCVQZ level, it increases by 0.39 kcal mol^{-1}. Thus, the core−valence effect at the CBS limit is 0.4 kcal mol^{-1}. This increases D_e to 97.4 and D_0 to 96.1 kcal mol^{-1}. This yields $\Delta_f H^0_{CCl,0K} = 102.5$ kcal mol^{-1}.

We have also calculated the bond energy for CCl_2 at this higher level of theory using the same procedure, and the results are also given in Table 5 and Figure 5. The value for D_e is 79.1 kcal mol^{-1} at the CBS limit for the R-CCSD(T) level of correlation. The core−valence correction is 0.25 giving a final value for $D_e = 79.4$ kcal mol^{-1}. The zero-point energy (ZPE) for CCl_2 can be taken from the experimental gas-phase values of $\nu_1 = 730$ cm^{-1} and $\nu_2 = 335.2$ cm^{-1} and the matrix value for $\nu_3 = 748$ cm^{-1}.[49] $ZPE_{CCl_2} = 2.6$ and $ZPE_{CCl} = 1.3$, giving $\Delta ZPE = 1.3$ kcal mol^{-1} which yields $D_0 = 78.1$ kcal mol^{-1} for the C−Cl bond strength in CCl_2. This is seen to be in very good agreement with our G2(MP2) value of 79.6 kcal mol^{-1} again casting doubt on the JANAF value. Use of our calculated $\Delta_f H^0_{CCl,0K}$ with D_0 in CCl_2 gives $\Delta_f H^0_{CCl_2,0K} = 53.0$ kcal mol^{-1}. This purely theoretical value is seen to be in good agreement with the previously mentioned experimental results of Kohn et al. ($\Delta_f H^0_{CCl_2,0K} = (50.7 \pm 2.0)$ kcal mol^{-1}).[24]

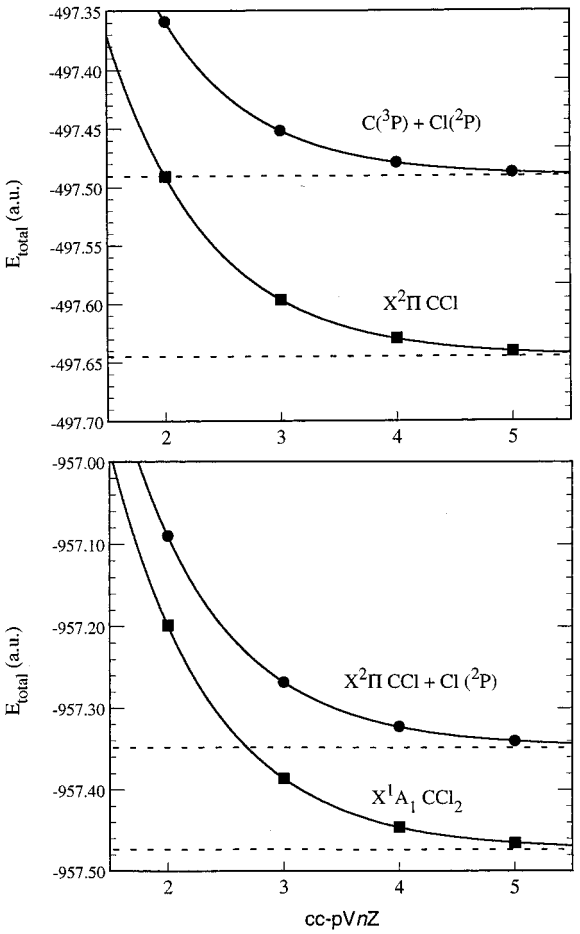

Figure 5. Plots of total energy (au) for predicting the values of D_e for (top) $X^2\Pi$ CCl and (bottom) X^1A_1 CCl_2 at the R-CCSD(T) level as a function of basis set size. cc-pVnZ is the n described in the text, and the curves are exponential fits to eq (9). Asymptotic values from the two top curves are −497.4908 and −497.6454, giving a difference of 0.1546 au = 97.0 kcal mol^{-1} as the CBS asymptotic limiting value. Similar values for the bottom curves are −957.3476 and −957.4740, giving 0.1264 au = 79.3 kcal mol^{-1} for D_e in CCl_2.

The data on which eq (5) is based are given in Table 3 and are plotted in Figure 6. These data can be used to also estimate an experimental value for the C−Cl bond strength in CCl_2 using semiempirical Troe calculations for the low-pressure limiting rate constants. Such calculations have been carried out with $E_0 = 79.6$ (G2(MP2)) and 78.1 (CBS) kcal mol^{-1}, and the $\langle\Delta E\rangle_{down}$ values necessary to fit these data are then ∞ and 4000 cm^{-1}, respectively, implying respective values for β_c of 1.0 and 0.45−0.66. E_0 values as low as 74 kcal mol^{-1} (with corresponding adjustment of $\langle\Delta E\rangle_{down}$) also fit the data. The best compromise, $E_0 = 76$ kcal mol^{-1} and $\langle\Delta E\rangle_{down} = 2000$ cm^{-1}, is shown in Figure 6 along with the k_3 values from Table 3. The Troe calculations with these parameters can be expressed to within 0.2% by: $k_3^{th} = 1.014 \times 10^{27}\ T^{-3.047}\ \exp(-40\ 149\ K/T)$ cm^3 mol^{-1} s^{-1} for $1550 \le T \le 2400$ K (this value is also listed in Table 1). On the basis of this experimental evidence, we conclude that the C−Cl bond strength in CCl_2 is much lower than previously proposed. Since it is unlikely that the experimental $\Delta_f H^0_{CCl_2,0K} = 50.7$ kcal mol^{-1} of Kohn et al.[24] is wrong by more than their stated error, ±2.0 kcal mol^{-1}, the $\Delta_f H^0_0$ for

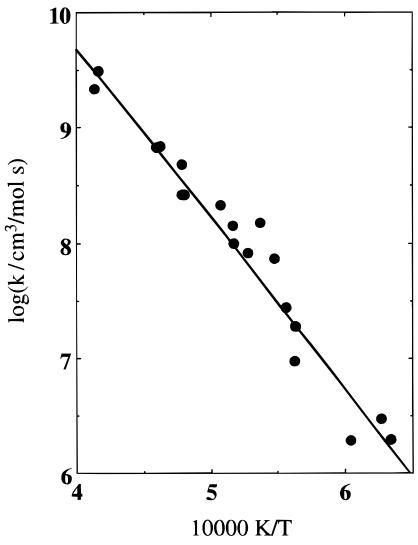

Figure 6. Arrhenius plot of second-order rate constants for $CCl_2 + Kr \rightarrow CCl + Cl + Kr$ (reaction (3) in Table 1) from the kinetics simulations to the ARAS data given in Table 3. The limiting low-pressure semiempirical Troe calculations were carried out with $E_0 = 76.0$ kcal mol^{-1} and $\langle\Delta E\rangle_{down} = 2000$ cm^{-1}, resulting in the solid line (see text).

CCl must be modified. With the experimental estimate, $E_0 = (76 \pm 2)$, and the Kohn et al. $\Delta_f H^0_{CCl_2,0K}$, $\Delta_f H^0_{CCl,0K} = (100 \pm 4)$ kcal mol^{-1} is obtained. Paulino and Squires[23] (whose value agrees with that of Kohn et al. within combined experimental errors) have pointed out that their $\Delta_f H^0_{CCl_2,0K}$ disagrees with that of Lias et al.;[50] however, Lias et al. have also estimated $\Delta_f H^0_{CCl,0K} = 104$ kcal mol^{-1}. Our experimental and theoretical $\Delta_f H^0_{CCl,0K}$ values both agree with Lias et al. and, with JANAF values for C(g) and Cl,[22] suggest respective values for the C−Cl bond strength at 0 K in CCl of (98.6 ± 4.0) and 96.1 kcal mol^{-1}.

The experimental and theoretical results can then be summarized giving respective $\Delta_f H^0_0$ values for CCl_2 of (50.7 ± 2.0) and 53.0 kcal mol^{-1}, and for CCl of (100 ± 4) and 102.5 kcal mol^{-1}. The agreement is remarkably good. Hence, degrading CCl_4 in four successive Cl-atom eliminations requires 68,[1,51] 63, ∼77, and ∼97 kcal mol^{-1} at 0 K, using the values derived here. This large value for the bond strength in CCl is then consistent with the present inference that this species is stable to dissociation even at ∼2500 K.

To understand the CCl_2 recombination results, we have carried out RRKM calculations (not shown) on the dissociation of C_2Cl_4 to give $2CCl_2$. With $\Delta_f H^0_{CCl_2,0K} = 50.7$[24] and $\Delta_f H^0_{C_2Cl_4,0K} = -2.8$,[22] $E_0 = 104.3$ (all in kcal mol^{-1}). Though our own G2(MP2)-like calculations[52] estimate the value at 114 kcal mol^{-1}, it seems clear from the work and arguments given by Paulino and Squires[23] that a lower value is warranted. The RRKM calculations were carried out with an assumed value for $\langle\Delta E\rangle_{down}$ of 400 cm^{-1}, giving, for $300 \le P \le 500$ Torr and $1200 \le T \le 1500$ K, $k^{th}_{diss} = 7.2 \times 10^{18} \exp(-44\,130\ \mathrm{K}/T)$ cm^3 mol^{-1} s^{-1}. Using the modified heats of formation, the equilibrium constant for $C_2Cl_4 \rightleftharpoons 2CCl_2$ was estimated as $K_{eq} = 5.0 \times 10^3 \exp(-50\,450\ \mathrm{K}/T)$ mol cm^{-3}. Combining the two expressions gives an estimate for the third-order recombination rate constant, k^{th}_4 in Table 1: $1.4 \times 10^{15} \exp(6320\ \mathrm{K}/T)$ cm^6 mol^{-2} s^{-1}. The experimental results summarized by eq (8) are roughly one-third to one-half of those implied by theory over the T-range 1200−1500 K. Hence, the values for k_4 in Table 3 are not in contradiction to theory.

The dissociative recombination process, reaction (2) in Table 1, can also be discussed using unimolecular theoretical arguments. Our potential energy surface evaluation for C_2Cl_4 dissociation to $2CCl_2$ at the CCSD(T)/cc-pvDZ//MP2/6-31G* level shows no hint of a saddle point. There should therefore be no barrier to recombination, and the initially formed molecule should be vibrationally hot by ∼104 kcal mol^{-1}. Furthermore, G2(MP2)-like calculations[53] show that $C_2Cl_3 + Cl$ formation should be lower lying than $2CCl_2$ by 18.2 kcal mol^{-1} and that the C−Cl bond strength in C_2Cl_3 should only be 25.3 kcal mol^{-1}. Therefore, once C_2Cl_3 is formed, it will rapidly dissociate to give the C_2Cl_2 product as in the overall reaction (2) of Table 1. However, Burcat and McBride[54] suggest that the C−Cl bond strength in C_2Cl_4 is 77 kcal mol^{-1} giving an even lower location for the exit channel at 28 kcal mol^{-1} below $2CCl_2$. The results for k_2 would then be expected to reflect the high-pressure limiting rate constant for CCl_2 recombination. It is therefore difficult to reconcile eq (4) with this thermodynamic analysis unless an exit barrier from C_2Cl_4* to $C_2Cl_3 + Cl$ exists. This seems unlikely. Part of the apparent activation energy in eq (4) may be due to effects of stabilization at lower temperatures; however, it is doubtful that this is the entire cause. It is worth noting that similar behavior has been directly observed in the recombination of CF_2;[55] i.e., an increasing rate constant with increasing temperature under limiting high-pressure conditions where little or no barrier to recombination can be justified by electronic structure calculations. Justification of reactions (11) and (12) in Table 1 is also difficult for two reasons: (1) the results on which eqs (6) and (7) are based are too limited, and (2) the molecular properties necessary for theoretically describing the processes are lacking, and thermodynamic quantities, even if they exist, are probably incorrect.

The most important experimental speculation from this scheme and, in particular, reactions (11) and (12), is that the main product at high temperatures will be C_2 radicals. If eqs (4)−(8) are correct, then $CHCl_3$ should be an excellent high-temperature source for preparing stable C_2 concentrations. The same should be true with CCl_4 where CCl_2 is surely a major product from CCl_3 decomposition.[1] In the absence of any other reactant, C_2 probably polymerizes giving the "white carbon" product (carbyne) that has already been identified by Frenklach and co-workers.[56] Lastly, at 1125 K, C_2 deposition on surfaces has already been shown to yield diamond films.[57] So, it is interesting to speculate what the transition temperature would be between the two mechanisms forming these distinct forms of carbon.

Acknowledgment. This work was supported by the U.S. Department of Energy, Office of Basic Energy Sciences, Division of Chemical Sciences, under Contract Nos.W-31-109-Eng-38 (Argonne) and DE-FGO2-85ER13384 (U. of Illinois). Also, this research was supported by the U.S. Department of Energy under Contract No. DE-AC06-76RLO 1830 (Division of Chemical Sciences, Office of Basic Energy Sciences and the Environmental Technology Partnerships Program). The Pacific Northwest National Laboratory is operated by Battelle Memorial Institute. We also thank the Scientitic Computing Staff, Office of Energy Research, U.S. Department of Energy for a grant of computer time at the National Energy Research Scientific Computing Center (Berkeley, CA).

References and Notes

(1) Michael, J. V.; Lim, K. P.; Kumaran, S. S.; Kiefer, J. H. *J. Phys. Chem.* **1993**, *97*, 1914.

(2) Kiefer, J. H.; Sathyanarayana, R.; Lim, K. P.; Michael, J. V. *J. Phys. Chem.* **1994**, *98*, 12278.

(3) Su, M.-C.; Kumaran, S. S.; Lim, K. P.; Michael, J. V.; Wagner, A. F.; Dixon, D. A.; Kiefer, J. H.; DiFelice, J. *J. Phys. Chem.* **1996**, *100*, 15827.

(4) Lim, K. P.; Michael, J. V. *J. Chem. Phys.* **1993**, *98*, 3919.

(5) Lim, K. P.; Michael, J. V. *Twenty-Fifth Symposium (International) on Combustion*, The Combustion Institute: Pittsburgh, PA, 1994; p 809.
(6) Lim, K. P.; Michael, J. V. *207th American Chemical Society Meeting, Fuel Chemistry Division*; **1994**, *39*, 131.
(7) Kumaran, S. S.; Lim, K. P.; Michael, J. V.; Wagner, A. F. *J. Phys. Chem.* **1995**, *99*, 8673.
(8) Kumaran, S. S.; Su, M.-C.; Lim, K. P.; Michael, J. V. *Chem. Phys. Lett.* **1995**, *243*, 59.
(9) Kumaran, S. S.; Su, M.-C.; Lim, K. P.; Michael, J. V.; Wagner, A. F. *J. Phys. Chem.* **1996**, *100*, 7533.
(10) Kumaran, S. S.; Su, M.-C.; Lim, K. P.; Michael, J. V.; Wagner, A. F.; Harding, L. B.; Dixon, D. A. *J. Phys. Chem.* **1996**, *100*, 7541.
(11) Kumaran, S. S.; Su, M.-C.; Michael, J. V. *Int. J. Chem. Kinet.* **1997**, *29*, 535.
(12) Schug, K. P.; Wagner, H. G.; Zabel, F. *Ber. Bunsen-Ges. Phys. Chem.* **1979**, *83*, 167.
(13) Semeluk, G. P.; Bernstein, R. B. *J. Am. Chem. Soc.* **1954**, *76*, 3793; **1957**, *79*, 46.
(14) Yano, T. *Bull. Chem. Soc. Jpn.* **1977**, *50*, 1272.
(15) Le Moan, G. *Compt. Rend.* **1962**, *254*, 2602.
(16) Benson, S. W.; Spokes, G. N. *Eleventh Symposium (International) on Combustion*; The Combustion Institute: Pittsburgh, PA, 1966; p 95.
(17) Herman, I. P.; Magnotta, F.; Buss, R. J.; Lee, Y. T. *J. Chem. Phys.* **1983**, *79*, 1789.
(18) Shilov, A. E.; Sabirova, R. D. *Russ. J. Phys. Chem.* (English Translation) **1960**, *34*, 408.
(19) Won, Y. S.; Bozzelli, J. W. *Combust. Sci. Technol.* **1992**, *85*, 345.
(20) Taylor, P. H.; Dellinger, B.; Tirey, D. A. *Int. J. Chem. Kinet.* **1991**, *23*, 1051.
(21) Vitovec, W.; Higgins, B. S.; Lucas, D.; Koshland, C. P.; Sawyer, R. F. *Proceedings of the Western States Section/Combustion Institute*, paper presentation, University of California at Davis, Davis, CA, March, 1994.
(22) Chase, M. W., Jr.; Davies, C. A.; Downey, J. R., Jr.; Frurip, D. J.; McDonald, R. A.; Syverud, A. N. *J. Phys. Chem. Ref. Data* **1985,** *14*, Supplement No. 1.
(23) Paulino, J. A.; Squires, R. R. *J. Am. Chem. Soc.* **1991**, *113*, 5573.
(24) Kohn, D. W.; Robles, E. S. J.; Logan, C. F.; Chen, P. *J. Phys. Chem.* **1993**, *97*, 4936.
(25) Kiefer, J. H.; Manson, A. C. *Rev. Sci. Inst.* **1981**, *52*, 1392.
(26) Michael, J. V. *Prog. Energy Combust. Sci.* **1992**, *18*, 327.
(27) Michael, J. V. in *Advances in Chemical Kinetics and Dynamics*; Barker, J. R., Ed.; JAI: Greenwich, 1992; Vol. I, p 47 for original references.
(28) Michael, J. V.; Sutherland, J. W. *Int. J. Chem. Kinet.* **1986**, *18*, 409.
(29) Michael, J. V. *J. Chem. Phys.* **1989**, *90*, 189.
(30) Clyne, M. A. A.; Nip, W. S. *J. Chem. Soc., Faraday II*, **1976**, *72*, 838.
(31) Whytock, D. A.; Lee, J. H.; Michael, J. V.; Payne, W. A.; Stief, L. J. *J. Chem. Phys.* **1977**, *66*, 290.
(32) Lim, K. P.; Michael, J. V. *J. Phys. Chem.* **1994**, *98*, 211.
(33) Seery, D. J.; Bowman, C. T. *J. Chem. Phys.* **1969**, *48*, 4314.
(34) Clyne, M. A. A.; Walker, R. F. *J. Chem. Soc., Faraday Trans. 1* **1973**, *69*, 1547.
(35) Jacobs, T. A.; Giedt, R. R. *J. Chem. Phys.* **1963**, *39*, 749.
(36) Dobbs, K. D.; Dixon, D. A. *J. Phys. Chem.* **1993**, *97*, 2085; **1994**, *98*, 12584.
(37) Regarding the theoretical implications at the CCSD(T)/CC level for the back-reaction, $\Delta E_{elec} = 61.8$ for reaction (1a) whereas $\Delta E_{elec} = 60.8$ kcal mol^{-1} between $CHCl_3$ and the transition state. The result that the transition state is lower in energy is likely due to basis set superposition error (BSSE) not being included for the products as compared to the reactant or transition state. This would lead to a stabilization of the products relative to the transition state. For example, for HCl + H at this level of calculation, the counterpoise estimate for BSSE is 1.4 kcal/mol (see ref 36). Inclusion of zero-point effects gives $\Delta H^0_{1a} = 55.9$ kcal mol^{-1}, the same energy as the transition state. On the basis of the value given below for $\Delta_f H^0_{CCl_2,0K} = 53.0$ kcal mol^{-1}, ΔH^0_{1a} 54.5 kcal mol^{-1}; i.e., 1.4 kcal mol^{-1} less than the value calculated at the CCSD(T)/TZ2PF level.
(38) Troe, J. *J. Chem. Phys.* **1977**, *66*, 4745; **1977**, 4758.
(39) Troe, J. *J. Phys. Chem.* **1979**, *83*, 114.
(40) Troe, J. *Ber. Bunsen-Ges. Phys. Chem.* **1983**, *87*, 161.
(41) Gilbert, R. G.; Luther, K.; Troe, J. *Ber. Bunsen-Ges. Phys. Chem.* **1983**, *87*, 169.
(42) Curtiss, L. A.; Raghavachari, K.; Pople, J. A. *J. Chem. Phys.* **1993**, *98*, 1293.
(43) (a) Bartlett, R. J. *J. Phys. Chem.* **1989**, *93*, 1697. (b) Kucharski, S. A.; Bartlett, R. J. *Adv. Quantum Chem.* **1986**, *18*, 281. (c) Bartlett, R. J.; Stanton, J. F. In *Reviews of Computational Chemistry*; Lipkowitz, K. B., Boyd, D. B., Eds.; VCH: New York, 1995; Vol. 5, p 65.
(44) (a) Dunning, T. H., Jr. *J. Chem. Phys.* **1989**, *90*, 1007. (b) Kendall, R. A.; Dunning, T. H., Jr.; Harrison, R. J. *J. Chem. Phys.* **1992**, *96*, 6796. (c) Woon, D. E.; Dunning, T. H., Jr. *J. Chem. Phys.* **1993**, *99*, 1914. (d) Peterson, K. A.; Kendall, R. A.; Dunning, T. H., Jr. *J. Chem. Phys.* **1993**, *99*, 1930. (e) Peterson, K. A.; Kendall, R. A.; Dunning, T. H., Jr. *J. Chem. Phys.* **1993**, *99*, 9790
(45) MOLPRO is a package of ab initio molecular orbital theory programs written by H.-J. Werner and P. J. Knowles with contributions from J. Almlöf, R. D. Amos, M. J. O. Deegan, S. T. Elbert, C. Hampel, W. Meyer, K. A. Peterson, R. M. Pitzer, A. J. Stone, P. R. Taylor, and R. Lindh.
(46) (a) Hampel, C.; Peterson, K. A.; Werner, H.-J. *Chem. Phys. Lett.* **1992**, *190*, 1. (b) Knowles, P. J.; Hampel, C.; Werner, H.-J. *J. Chem. Phys.* **1994**, *99*, 5219. (c) Deegan, M. J. O.; Knowles, P. J. *Chem. Phys. Lett.* **1994**, *227*, 321.
(47) (a) Xantheas, S. S.; Dunning, T. H., Jr. *J. Phys. Chem.* **1993**, *97*, 18. (b) Feller, D. J. *Chem. Phys.* **1992**, *96*, 6104.
(48) (a) Woon, D. E.; Dunning, T. H., Jr. *J. Chem. Phys.* **1995**, *103*, 4572. (b) Peterson, K. A.; Dunning, T. H., Jr. Manuscript in preparation.
(49) Jacox, M. E. *J. Phys. Chem. Ref. Data* **1994**, Monograph #3.
(50) Lias, S. G.; Karpas, Z.; Liebman, J. F. *J. Am. Chem. Soc.* **1985**, *107*, 6089.
(51) Hudgens, J. W.; Johnson, R. D., III; Timonen, R. S.; Seetula, J. A.; Gutman, D. *J. Phys. Chem.* **1991**, *95*, 4400.
(52) Due to disk space limitations the MP2/6-311-G+(3df,2p) evaluations were replaced with MP2/6-311-G+(2df,2p) evaluations.
(53) Due to disk space limitations the MP2/6-311-G+(3df,2p) energy was estimated in terms of a combination of MP2/6-311-G+(2df,2p) and MP2/6-311-G(3df,2p) evaluations for the energetics of C_2Cl_3 relative to $2CCl_2$.
(54) Burcat, A.; McBride, B. *Ideal Gas Thermodynamic Data for Combustion and Air-Pollution Use*; Technion Aerospace Report TAE732, Technion, Tel Aviv, Jan. 1995.
(55) Murrels, T. P.; Battin-Leclerc, F.; Hayman, G. D. *13th International Symposium on Gas Kinetics*; University College Dublin, paper A10, 1994; p 23.
(56) Frenklach, M. *Combust. Sci. Technol.* **1990**, *74*, 283 and references therein.
(57) Gruen, D. M.; Zuiker, C. D.; Krauss, A. R.; Pan, X. *J. Vac. Sci. Technol.* **1995**, *13*, 1628. Redfern, P. C.; Horner, D. A.; Curtiss, L. A.; Gruen, D. A. *J. Phys. Chem.* **1996**, *100*, 11654.